RSC Advances

ROYAL SOCIETY OF CHEMISTRY

www.rsc.org/advances

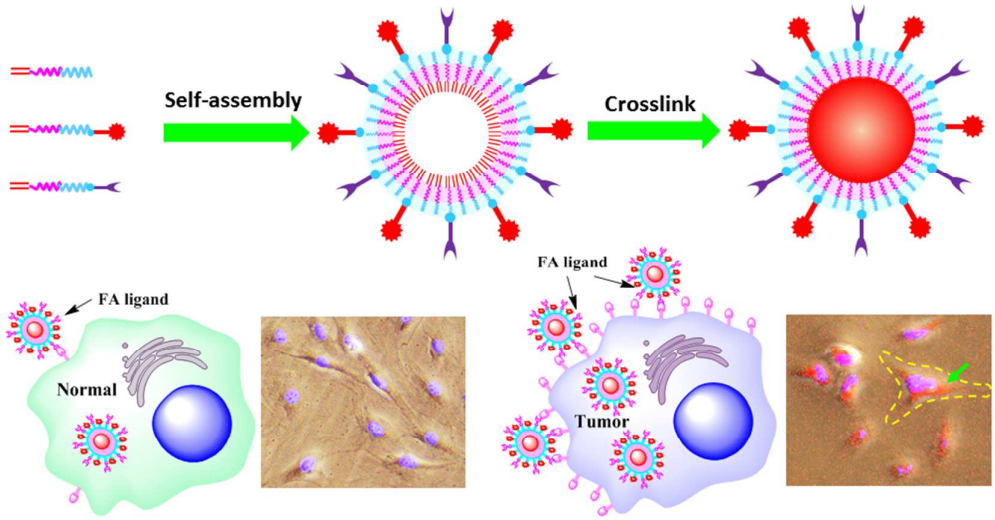

Novel crosslinkable self-assembled PPF-PLGA-PEG nanoparticles with fluorescent RhB probes and FA ligands for targeted cancer imaging and potential drug delivery.

RSC Advances

RSCPublishing

Paper

Biodegradable and crosslinkable PPF-PLGA-PEG self-assembled nanoparticles dual-decorated with folic acid ligands and rhodamine B fluorescent probes for targeted cancer imaging

Cite this: DOI: 10.1039/xoxxoooooox

Received ooth March 2015,
Accepted ooth March 2015

DOI: 10.1039/xoxxoooooox

www.rsc.org/

Xifeng Liu,[ab] A. Lee Miller II,[ab] Michael J. Yaszemski[ab] and Lichun Lu[*ab]

Novel biodegradable and crosslinkable copolymers of hydrophobic poly(propylene fumarate)-*co*-poly(lactic-*co*-glycolic acid) (PPF-PLGA) linked with hydrophilic poly(ethylene glycol) (PEG), namely PPF-PLGA-PEG, were developed and fabricated into core-shell nanoparticles through self-assembly and photocrosslinking. A fluorescent probe, rhodamine B (RhB), was conjugated to the end of the copolymer chain (PPF-PLGA-PEG-RhB), which allows tracking of the nanoparticles through visualizing the fluorescence probe. Folic acid (FA) ligand was conjugated to another series of chains (PPF-PLGA-PEG-FA) for targeted delivery of the nanoparticles to the tumor sites by binding to the ubiquitously overexpressed FA receptors on tumor cells. Our results showed that PPF-PLGA-PEG nanoparticles incorporated with RhB fluorescence probes and FA tumor binding ligands have specific cancer cell targeting and imaging abilities. These crosslinkable nanoparticles are potentially useful to serve as a platform for conjugation of fluorescence probes as well as various antibodies and peptides for cancer targeted imaging or drug delivery.

Introduction

Nanotechnology has received intensive attention in the biomedicine fields ranging from tissue engineering to drug delivery.[1] In the past decades, various nano systems have been developed for biomedical applications, e.g., liposomes,[2] nanoparticles,[3] quantum dots[4] and dendrimers.[5] The fabrication of nanoparticles from amphiphilic copolymers, inside which contain a hydrophobic segment and a hydrophilic segment, have been studied extensively in applications from cell imaging to drug and gene delivery. For the hydrophobic component, the poly(ε-caprolactone) (PCL),[6-8] poly(2-hydroxyethyl methacrylate) (pHEMA),[9] poly(propylene fumarate) (PPF)[10] and their copolymers[11,12] have been acknowledged to have excellent biocompatibility. With advantages of tunable mechanical properties, PPF and its copolymers/blends have also been evaluated extensively for various tissue engineering applications.[13] In addition, poly(lactic acid) (PLA), poly(glycolic acid) (PGA) and their copolymer poly(lactic-co-glycolic acid) (PLGA) were reported to have favorable chemical properties such as controlled biodegradability through hydrolysis.[14] For the hydrophilic segment, poly(ethylene glycol) (PEG) is one of the most widely applied polymer because of its excellent hydrophilicity and biocompatibility.[15]

To achieve cancer-specific targeting abilities, large categories of targeting ligands have been developed, including aptamers, folic acid, antibodies and peptides.[16] Folic acid is generally transported into the cells by binding to the cellular membrane folic acid receptors, which are overexpressed in a majority of human cancer cells.[17] Fluorescent probes, e.g., fluorescein isothiocyanate (FITC) and rhodamine B (RhB), are promising markers for cell detection because of their high sensitivity.[18] However, drawbacks of conventional fluorescent dyes include easy contamination, troublesome in handling due to their small molecule weight, and nonspecific staining of tissues.[19] The conjugation of these small molecule fluorescent dyes to polymeric chains thus becomes a promising route to overcome these drawbacks. Furthermore, polymer-fluorescence probe combination has unique advantages, such as favorable mechanical properties and tissue specific targeting abilities by conjugation with targeting ligands, which makes them attractive for applications in fluorescent chemo-sensors, molecular thermometers and drug delivery systems.[19]

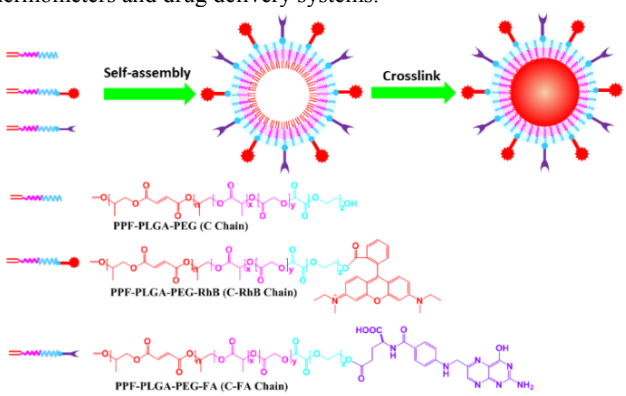

Fig. 1 Scheme of the self-assembly and crosslinking of PPF-PLGA-PEG micelle system.

Taking these factors into consideration, here in this study we present a novel biodegradable and crosslinkable PPF-PLGA-PEG self-assembled core-shell nanoparticle system conjugated with highly luminescent RhB probes and FA tumor targeting ligands for cancer targeted tracking, imaging and potential anticancer drug delivery. PPF-PLGA triblock copolymers were synthesized by a ring opening reaction of D,L-lactide and glycolide monomer (50:50, molar ratio) using PPF as initiator. Purified PPF-PLGA was then coupled with hydrophilic PEG chains to make amphiphilic PPF-PLGA-PEG block copolymers. RhB and FA were then conjugated to obtain PPF-PLGA-PEG-RhB and PPF-PLGA-PEG-FA by the esterification reaction between hydroxyl groups in PPF-PLGA-PEG polymer and carboxyl groups on RhB and FA molecules, respectively. The PPF-PLGA-PEG nanoparticles incorporated with RhB fluorescence probe and FA tumor targeting ligand were then formed by self-assembly in aqueous solution and crosslinked under UV light, as demonstrated in Fig. 1. These crosslinked FA and RhB dual-decorated PPF-PLGA-PEG nanoparticles exhibited excellent cancer cell targeting and imaging ability.

Experimental

Materials and characterization

Glycolide (1,4-dioxane-2,5-dione), D,L-lactide (3,6-dimethyl-1,4-dioxane-2,5-dione), fumaryl chloride, propylene glycol, dimethyl sulfoxide (DMSO), *N,N′*-dicyclohexylcarbodiimide (DCC, ⩾99%), 4-(dimethylamino) pyridine (DMAP, ⩾ 99%), RhB and folic acid (FA) were purchased from Sigma Aldrich Co. (Milwaukee, WI) and used as receive. Solvents (reagent grade) were purchased from Fisher (Pittsburgh, PA). Anhydrous methylene chloride (CH_2Cl_2) was dried over calcium hydride (CaH_2) and distilled prior to use. All other chemicals/reagents were purchased from Sigma or Fisher and used as receive unless noted otherwise.

The chemical structures of obtained polymers were characterized by ^{1}H NMR spectroscopy (300 MHz Varian NMR) using $CDCl_3$ or DMSO-d_6 solvent. Molecular weights of polymers synthesized were analyzed by gel permeation chromatography (GPC) method on a Viscotek GPCMax/VE 2001 GPC machine (Malvern Instruments, Inc.) equipped with a model 2410 refractive index detector. Tetrahydrofuran (THF) was selected as eluent in this process (flow rate: 1 mL min^{-1}). Universal calibration system was applied to calculate the absolute molecular weights of polymers.

Synthesis of PPF-PLGA copolymer

PPF was synthesized from 1,2-propylene glycol and diethyl fumarate monomers using zinc chloride as catalyst, as described in our previous report.[20] Briefly, 1,2-propylene glycol (34 g), diethyl fumarate (26 g), crosslinking inhibitor hydroquinone (33 mg), and catalyst zinc chloride (0.2 g) were mixed together and heated to 100 °C for 1 h. The temperature was then gradually increased to 150 °C for another 7 h to produce fumaric diester. Distillation under nitrogen was exerted to the reaction mixture to remove the ethanol and propylene glycol byproducts. Synthesized fumaric diester was further polycondensed to obtain linear PPF chains with hydroxyl end groups. Dried PPF (11 g) was copolymerized with D,L-lactide (28.8 g) and glycolide (23.2 g) monomer by a ring opening reaction at 140 °C for 24 h using stannous octoate ($Sn(Oct)_2$) as catalyst, according to the previous report.[21] Obtained PPF-PLGA copolymers were fully dissolved in methylene chloride, then precipitated in diethyl ether and fully dried under vacuum.

Synthesis of PPF-PLGA-PEG copolymer

PPF-PLGA (10 g, 1 m mol) was dissolved in 50 mL of anhydrous CH_2Cl_2. Excess oxalyl chloride (1 mL, 12 m mol) was added to 50 mL of anhydrous CH_2Cl_2 in a 250 mL flask. Potassium carbonate (K_2CO_3, 10 g) was added as proton scavenger. PPF-PLGA/CH_2Cl_2 solution was then added dropwise to the flask. The reaction mixture was stirred at ambient temperature for 24 h, then centrifuged at 2000 rpm for 5 min to remove K_2CO_3 solids. CH_2Cl_2 solvent and excess oxalyl chloride was removed by rotary evaporation under reduced pressure to obtain PPF-PLGA-COCOCl. Excess dried HO-PEG-OH (M_n = 1 000 g mol^{-1}, 13 g, 13 m mol) in 50 mL of anhydrous CH_2Cl_2 was then mixed with PPF-PLGA-COCOCl. Pyridine (1 mL) and DMAP (50 mg) were added to the flask. Potassium carbonate (K_2CO_3, 10 g) was added as proton scavenger. The reaction mixture was stirred at ambient temperature for 24 h, then centrifuged at 2 000 rpm for 5 min to remove K_2CO_3 solids. The polymer mixture was then precipitated in excess methanol (CH_3OH, 100 mL) and stirred for 1 h. The obtained polymer mixture was dissolved in CH_2Cl_2 (20 mL), then precipitated in excess methanol (100 mL). This purification process was repeated for at least 5 times to remove the unreacted HO-PEG-OH, as reported previously.[22]

Synthesis of fluorescent PPF-PLGA-PEG-RhB chains

Hydroxyl-terminated PPF-PLGA-PEG (1.1 g, 0.1 m mol), RhB (25.0 mg, 0.052 m mol), dehydrant DCC (142.0 mg, 0.69 mmol), and catalyst DMAP (10.0 mg, 0.08 mmol) were dissolved in 20 mL anhydrous dimethyl sulfoxide (DMSO). After stirring at ambient temperature for 24 h, the reaction mixture was filtrated to remove solid *N,N′*-dicyclohexylurea (DCU). Subsequently, the filtrate was precipitated and washed in 100 mL methanol/diethyl ether (1/15, v/v) for five times. The unreacted RhB was fully dissolved in methanol and removed in the washing process. Precipitated PPF-PLGA-PEG-RhB chains were then dried under vacuum for 24 h, and kept at -20 °C prior to use.

Synthesis of functionalized PPF-PLGA-PEG-FA chains

Hydroxyl-terminated PPF-PLGA-PEG (1.1 g, 0.1 m mol), FA (25.0 mg, 0.057 m mol), dehydrant DCC (142.0 mg, 0.69 mmol), and catalyst DMAP (10.0 mg, 0.08 mmol) were dissolved in 20 mL anhydrous DMSO. The mixture was stirred at room temperature for 24 h, then the solution was filtrated to remove DCU. Next, the filtrate was precipitated and washed in 100 mL methanol/diethyl ether (1/15, v/v) for five times to remove unreacted FA molecules in the mixture. Precipitated PPF-PLGA-PEG-FA chains were then dried under vacuum for 24 h, and kept in -20 °C before usage. All of the synthesis routes are demonstrated in Fig. 2. For ease of reference, PPF-PLGA-PEG chains are abbreviated as C (for copolymer), PPF-PLGA-PEG-RhB as C-RhB, and PPF-PLGA-PEG-FA as C-FA.

Formation of polymer micelles

Micelles were prepared by addition of 10 mL of distilled water to 1 mL acetone solution containing 5 mg polymer (PPF-PLGA-PEG, PPF-PLGA-PEG-RhB, or PPF-PLGA-PEG-FA) under stirring at room temperature. Stirring was continued for another 10 min to stabilize the micelles and facilitate the evaporation of acetone solvent. Residual acetone was fully removed by rotary evaporation under reduced pressure. The obtained aqueous solution was slightly cloudy resembling diluted milk, substantiating the formation of polymer micelles in the solution. Final micelle concentration was 0.5 mg ml^{-1}. Three types of particle were prepared, i.e., PPF-PLGA-PEG (C), PPF-PLGA-PEG/PPF-PLGA-PEG-RhB (C/C-RhB, 20wt% C-RhB) and PPF-PLGA-PEG/PPF-PLGA-PEG-RhB/PPF-PLGA-PEG-FA (C/C-RhB/C-FA, 20wt% C-RhB, 20wt% C-FA). Dynamic light scattering (DLS) was performed using Zetasizer Nano ZS (Malvern Instruments) to determine the mean hydrodynamic radii of the formed micelles.

Crosslinking of polymer micelles

The biocompatible UV initiator, 1-[4-(2-hydroxyethoxy)-phenyl]-2-hydroxy-2-methyl-1-propanone (Irgacure 2959, Ciba Specialty Chemicals, Tarrytown, NY), has been widely used to photocrosslink hydrogels for tissue engineering applications. Here, Irgacure 2959 was employed as a photo-initiator to crosslink the PPF based polymeric micelles. Acetone solution of Irgacure 2959 (50 μL, 10 mg/mL) was introduced to 1 mL acetone solution dissolved with polymers (5 mg/mL), resulting in a final Irgacure 2959/polymer concentration of 10.0 wt%. Then 10 mL of distilled water was added to the acetone solution under stirring. Stirring was continued for 10 min to stabilize the micelles and residual acetone was removed by rotary evaporation. The obtained aqueous micelle solution was irradiated under 365 nm UV light at an intensity of ~8 mW cm^{-2} (Black-Ray Model 100AP, Upland, CA) for 3 min to yield crosslinked nanoparticles, as referred to a previous report.[23] The sizes of the formed nanoparticles were detected using DLS and the morphology was characterized using scanning electron microscopy (SEM; S-4700, Hitachi Instruments, Tokyo, Japan) at a voltage of 3.0 kV.

Cell viability in the presence of polymer micelles

MC3T3 cells and HeLa cells were used as examples of normal and tumor cells, respectively. The cells were separately seeded at a density of 10 000 cells cm^{-2} in 48-well tissue culture polystyrene (TCPS) plates and cultured for 24 h in Dulbecco's Modified Eagle's medium (DMEM) supplemented with L-glutamine (2 mM), penicillin (100 U ml^{-1}), streptomycin (0.1 mg ml^{-1}), and 10% heat-inactivated fetal bovine serum (FBS) to allow cell attachment. Crosslinked C, C/C-RhB, and C/C-RhB/C-FA micelles were prepared, centrifuged, and re-suspended in DMEM solution to obtain various concentrations of nanoparticles. The cells were then incubated with crosslinked C, C/C-RhB, or C/C-RhB/C-FA nanoparticles at varied concentrations of 1, 2, 3, 4 and 5 mg mL^{-1}. Wells seeded with cells at the same density without nanoparticle addition were used as positive controls and empty wells as negative controls. Cells were then cultured at 37 °C in a humidified condition of 95% air and 5% CO_2 for 3 days. Cell numbers were determined using MTS assay solutions (CellTiter 96 Aqueous One Solution, Promega, Madison, WI) using the UV-vis absorbance microplate reader at the wavelength of 490 nm, according to the manufacturer's protocol. The cell viability (%) was calculated by comparing the absorbance of each well with that of positive control wells (set as 100%).

Cellular uptake of polymer micelles

MC3T3 cells and HeLa cells were seeded at a density of 10 000 cells cm^{-2} in 48-well TCPS plates and cultured for 24 h for cells in DMEM as described above. Crosslinked C, C/C-RhB, and C/C-RhB/C-FA micelles were prepared, centrifuged, and re-suspended in PBS solution to obtain a final concentration of 5 mg/ml micelles in PBS. The cells were then washed with warm PBS and incubated with a suspension (100 μl) of crosslinked micelles (5 mg ml^{-1}) for 30 min in a humidified condition of 95% air and 5% CO_2 at 37 °C. Afterwards, the cells were washed three times with PBS to remove unattached micelles and fixed with 4% paraformaldehyde at room temperature for 10 min. Cells were then washed three times to remove paraformaldehyde. Cell nuclei were stained with DAPI (4',6-diamidino-2-phenylindole) over a period of 2 min. Cells was observed and imaged using Axiovert 25 Zeiss light microscope (Carl Zeiss, Germany).

Results and discussion

PPF, PPF-PLGA, PPF-PLGA-PEG synthesis

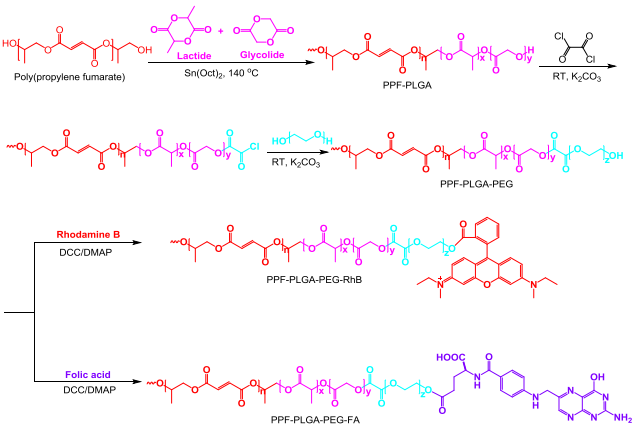

Fig. 2 Synthesis routes of multiple polymer chains for the micelle system.

Biodegradable and crosslinkable PPF was synthesized from diethyl fumarate and 1,2-propylene glycol, which are biologically compatible. The number average molecular weight (M_n), weight average molecular weight (M_w) and polydispersity index (PDI) for the synthesized PPF product were determined by GPC using THF as eluent to be M_n = 1 900 g mol^{-1}, M_w = 4 500 g mol^{-1}, and PDI = 2.4.

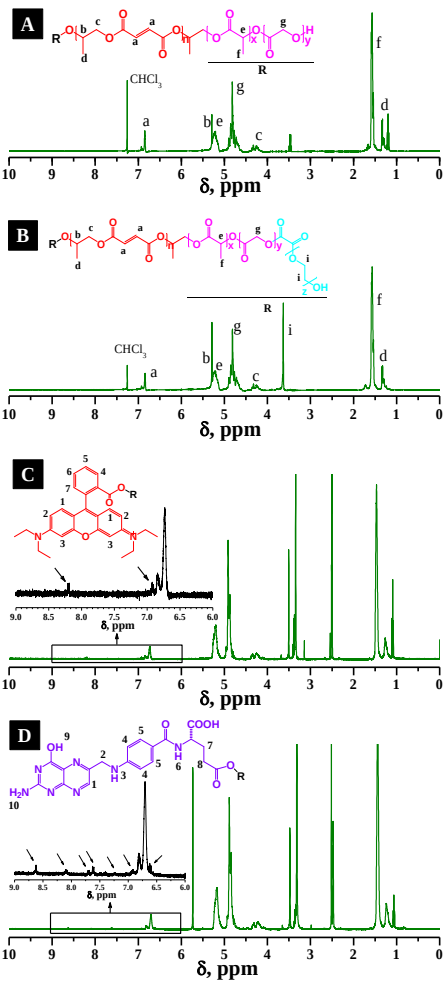

Fig. 3 ^{1}H NMR spectra of (A) PPF-PLGA (in $CDCl_3$); (B) PPF-PLGA-PEG (in $CDCl_3$); (C) PPF-PLGA-PEG-RhB (in DMSO-d_6); (D) PPF-PLGA-PEG-FA (in DMSO-d_6).

PPF-PLGA triblock copolymers were synthesized by ring opening polymerization of D,L-lactide and glycolide monomer (50:50, molar ratio) using PPF as initiator. Purified PPF-PLGA was calibrated by GPC to have M_n = 10 800 g mol^{-1}, M_w = 31 400 g mol^{-1} and *PDI* = 2.9. PPF-PLGA and PEG were successfully coupled using oxalyl chloride. The resulting copolymer, PPF-PLGA-PEG, had a yield ratio of approximately 80% of the theoretical mass. The M_n, M_w and *PDI* for the synthesized PPF-PLGA-PEG product were determined to be 12 200 g mol^{-1}, 30 000 g mol^{-1} and 2.4, respectively. Chemical shifts in ^{1}H NMR spectra of PPF-PLGA and PPF-PLGA-PEG (Fig. 3A and B) showed functional groups of the corresponding polymers, confirming a success of polymer synthesis.

RhB fluorescence probe and FA ligand conjugation

Following the synthesis of PPF-PLGA-PEG, fluorescent PPF-PLGA-PEG-RhB was prepared via DCC coupling. ^{1}H NMR spectra in Fig. 3C obtained using DMSO-d_6 as solvent displayed corresponding resonance peaks for protons on the RhB residue. Specifically, the corresponding peaks located at 6.90 to 8.3 ppm were assigned to the aromatic ring protons on RhB, which indicated that RhB residue was successfully conjugated to the PPF-PLGA-PEG chain, consistent with previous reports.[24]. The synthesized PPF-PLGA-PEG-RhB had a M_n of 13 200 g mol^{-1}, a M_w of 21 600 g mol^{-1}, and a *PDI* of 1.6. It appeared as a red solid with a yield ratio of approximately 80%. PPF-PLGA-PEG-FA conjugation was obtained by the esterification reaction between hydroxyl groups in PPF-PLGA-PEG and carboxyl groups on folic acid. The ^{1}H NMR resonance spectrum of obtained PPF-PLGA-PEG-FA copolymer were determined using DMSO-d_6 as solvent and displayed in Fig. 3D. The multiple resonance peaks between 8.60 and 6.57 ppm were assigned to the corresponding protons of FA aromatic rings.[24] The synthesized PPF-PLGA-PEG-FA had a M_n of 18 400 g mol^{-1}, a M_w of 49 700 g mol^{-1}, and a *PDI* of 2.7. It appeared as a yellow solid with a yield ratio of approximately 80-90%.

Nanoparticle formation and cytotoxicity

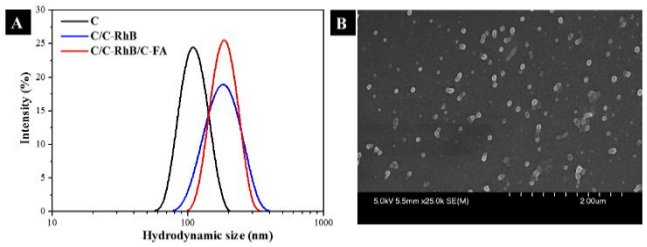

Fig. 4 (A) The hydrodynamic sizes for crosslinked C, C/C-RhB and C/C-RhB/C-FA nanoparticles. (B) SEM images of crosslinked C nanoparticles.

The amphiphilic nature of hydrophobic-hydrophilic block copolymers provides an opportunity to form micelles at nanoscale. The hydrophobic PPF-PLGA segment was expected to assemble into a hydrophobic core while the hydrophilic PEG chain together with the conjugated RhB or FA components form the shell of the micelles. Size distributions of C, C/C-RhB/C-FA nanoparticle were determined by DLS and visualized with SEM (Fig. 4). Hydrodynamic size had average values of 108.9 ± 0.4, 169.1 ± 1.3 and 175.9 ± 2.5 (Fig. 4A) for crosslinked C nanoparticle, C/C-RhB and C/C-RhB/C-FA nanoparticles, respectively. SEM images were consistent with the DLS measurement results, as demonstrated by the crosslinked C nanoparticles in Fig. 4B.

Cytotoxicity of self-assembled polymeric nanoparticles was evaluated using normal osteoblast MC3T3 cells and HeLa cancer cells over 72 h. The polymer nanoparticles showed no obvious cytotoxicity to either cell type as indicated by the high viability of cells cultured in the presence of nanoparticles at different concentrations for 3 days (Fig. 5). It is reasonable for the low cytotoxicity of PPF-PLGA-PEG copolymers since the PPF, PLGA and PEG segments in the backbone chain are all biocompatible.

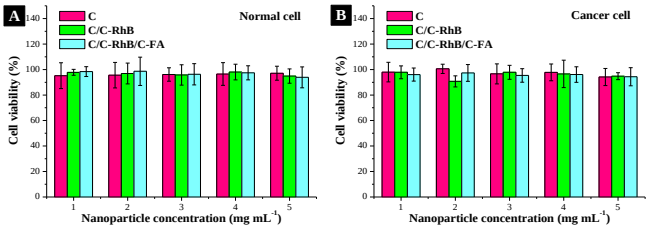

Fig. 5 Cell viability of (A) normal and (B) cancer cells cultured for 3 days in the presence of C, C/C-RhB and C/C-RhB/C-FA nanoparticles at various concentrations.

Cellular targeting and imaging

Since RhB exhibits inherent fluorescence, the targeted bonding of nanoparticles to tumor cells can be directly monitored by fluorescence microscope using RhB residue conjugated onto nanoparticle as probes. The tracking and imaging were performed on both normal osteoblast MC3T3 cells and HeLa cancer cells. After an incubation of 30 min with C, C/C-RhB, or C/C-RhB/C-FA nanoparticles, comparison of detectable results for cancer cells and normal cells were observed and displayed in Fig. 6 and Fig. 7, respectively.

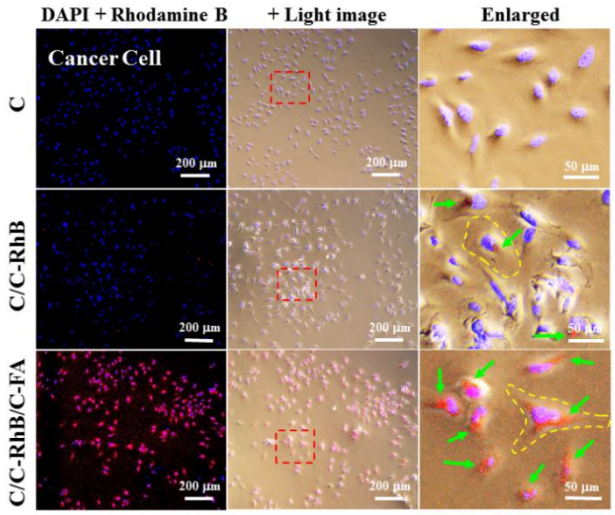

Fig. 6 Cellular uptake of crosslinked nanoparticles with or without FA ligand in HeLa cancer cells. Green allows point to the fluorescence from nanoparticles.

As seem from Fig. 6, the C nanoparticle without conjugation of RhB fluorescence probe and FA tumor binding ligand, which was used as a negative contrast group, had no detectable fluorescence. For the C/C-RhB nanoparticle conjugated with fluorescence marker whereas no conjugation of FA, limited fluorescence dots could be detected. This result showed that the incorporation of RhB fluorescence probe successfully achieved a tracking ability for the nanoparticles. This RhB imaging results was consistent with the report from other groups.[25] However, without the FA binding ligands, the limited fluorescence dots imaged were largely due to the passive uptake of nanoparticles through cellular membranes during cell activities. After the incorporation of FA conjugated chains, the C/C-RhB/C-FA

copolymer nanoparticle could be firmly adhered to HeLa cancer cells and clearly imaged (Fig. 6, last row). Consistent with reports from other groups,[26] our results demonstrated that the conjugation of FA to nanoparticles is an effective way to enhance the cellular uptake through binding between FA and cell surface FA receptors. The results also proved that the covalent linking of folic acid via its carboxyl group to hydroxyl group in PPF-PLGA-PEG molecule retained the FA binding function.

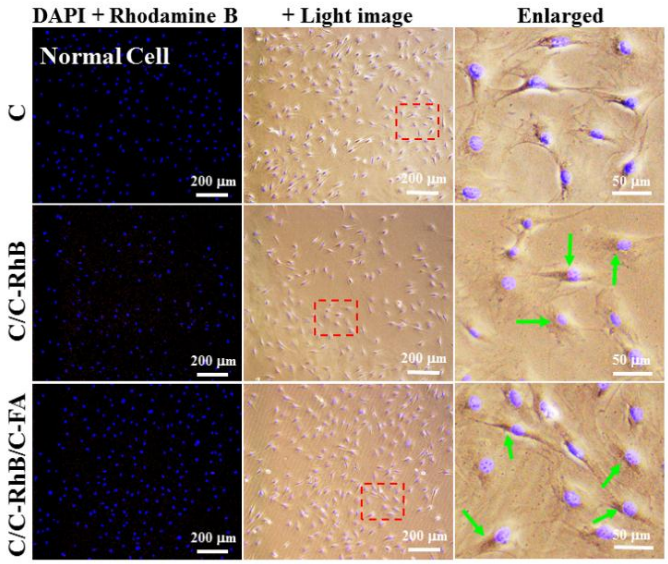

Fig. 7 Cellular uptake of crosslinked nanoparticles with or without FA ligand in normal cells. Green allows point to the fluorescence from nanoparticles.

For normal cells, no significance difference in fluorescence signal was detected for C/C-RhB and C/C-RhB/C-FA nanoparticles with or without incorporation of FA ligand (Fig. 7). This is caused by the limited expression of FA receptors on normal cells. The limited fluorescence signals detected, however, were largely contributed by the cellular membrane's passive uptake of nanoparticles during cell activities, the same reason as for no FA conjugated C/C-RhB nanoparticle in cancer cells.

Statistical analysis and mechanism

The percentage of normal MC3T3 cells and HeLa cancer cells showing fluorescence of Rhodamine B were analysed and summarized in Fig. 8. One-way analysis of variance (ANOVA) was performed for groups with or without FA ligands using the OriginLab software and $p < 0.01$ was considered significant.

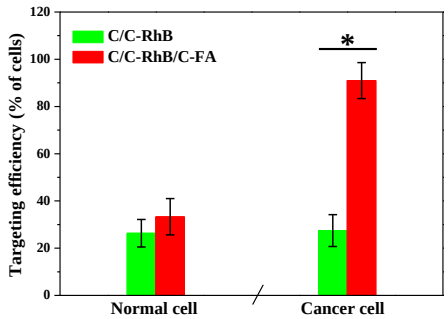

Fig. 8 Percentage of cells showing fluorescence of Rhodamine B conjugated in nanoparticle. * $p < 0.01$.

It can be clearly seen from the graph that a significantly higher number (p <0.01) of HeLa cancer cells showed fluorescence when incubated with FA incorporated C/C-RhB/C-FA nanoparticles. For C/C-RhB nanoparticle without FA ligand, a percentage of ~30% cells showed detectable fluorescence. However, the percentage value increased to ~ 90% after the introduction of FA conjugated chains. For normal cells, a percentage of ~30% cells were determined to have detectable fluorescence. No statistical differences were found in cellular uptake of nanoparticles with or without FA ligand for normal cells.

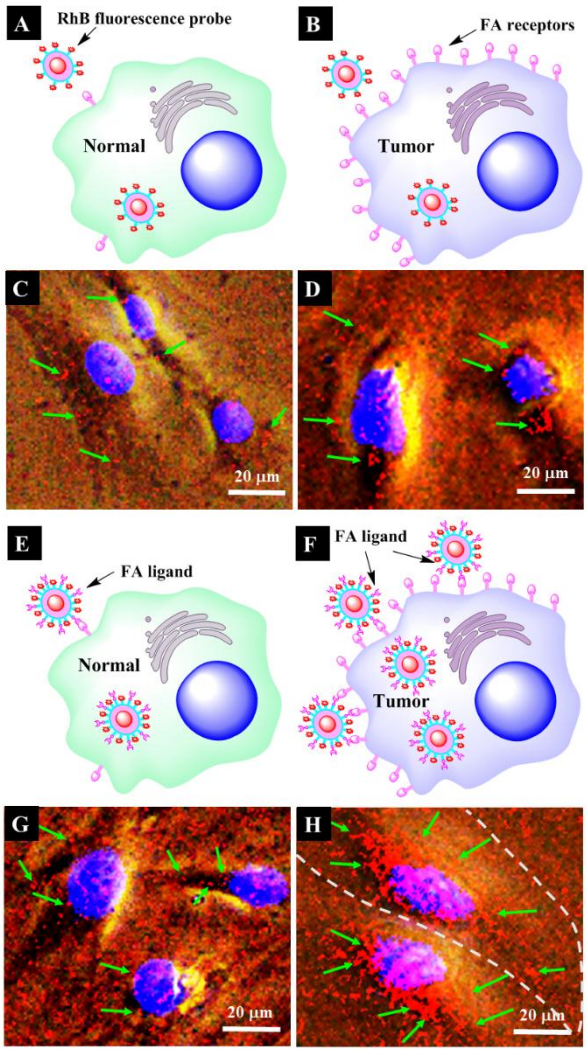

Fig. 9 Schematic illustration and corresponding experimental images of the cancer targeting strategy by polymer micelles. Micelles without FA ligand showed similar uptake into (A) normal cell and (B) cancer cell, and the real images observed in these cases are presented in (C) and (D), respectively. On the other hand, micelles conjugated with FA showed differential uptake into (E) normal cell and (F) cancer cells, as evidenced by fluorescence images demonstrated in (G) and (H), respectively. Green allows point to the fluorescence from nanoparticles.

The fluorescence results showed a difference in cellular uptake ability of FA conjugated nanoparticles in normal and cancer cells. The mechanisms causing these phenomena, however, are believed to originate from the folate receptor-mediated targeting in cancer cells. FA receptor is overexpressed in a large variety of human cancer cells, e.g., cancer cells originating from nasopharyngeal carcinoma,

ovary, cervix, pancreas, breast, and myeloid leukemia.[27] As illustrated in Fig. 9A-D, when C/C-RhB nanoparticles without FA conjugation meet the cell, cellular membrane passively take a small amount of nanoparticles whereby resulting a limited amount of fluorescence signals.

When the FA residue chain was incorporated to make the C/C-RhB/C-FA nanoparticle, for normal cells with limited FA receptor expression, the passive uptake is still the main route for taking foreign particles (Fig. 9E and G). However, when C/C-RhB/C-FA nanoparticles meet cancer cells with overexpressed FA receptors on the cell membrane, FA residues actively bind to the FA receptors (Fig. 9F and H). This FA receptor-mediated binding keeps the nanoparticle on the cell membrane and initiates the receptor-mediated endocytosis.[28] Hence, the prevalence of folate receptor overexpression on HeLa cells, or other types of tumor cells, makes it a specific marker for FA conjugated polymeric micelles to recognize and target.[29] Our newly developed PPF-PLGA-PEG system conjugated with cancer targeting FA ligand thus gains promise in anticancer drug delivery through active FA-FA receptor binding.

Conclusions

In summary, we have developed a facile method to fabricate biodegradable and self-assembled PPF-PLGA-PEG nanoparticles with RhB luminescent probes and a FA tumor binding ligand for targeted tracking, imaging and potential anticancer drug delivery to cancer cells. The conjugation of RhB and FA molecules to PPF-PLGA-PEG chains through esterification reaction of carboxyl groups and hydroxyl groups retained the functions of RhB and FA ligands. This conjugation method using DCC/DMAP coupling thus provides an effective route for linking fluorescence probe and tumor targeting ligand to polymer chains terminated with hydroxyl groups. Compared with C/C-RhB nanoparticles, significantly increased uptake of C/C-RhB/C-FA nanoparticles in cancer cells was observed owing to the active binding of FA ligands to cell surface FA receptors. The newly synthesized PPF-PLGA-PEG nanoparticles conjugated with luminescent probes and FA tumor binding ligands therefore hold promise in targeted therapy of various cancer cell types that overexpressing FA receptors, including brain, colon, lung, ovary, uterus and kidney.

Acknowledgements

This work was supported by the Mayo Foundation and NIH grants R01 AR56212 and R01 EB03060.

Notes

[a] *Department of Orthopedic Surgery, Mayo Clinic, Rochester, MN 55905, USA. Email: Lu.Lichun@mayo.edu*
[b] *Department of Physiology and Biomedical Engineering, Mayo Clinic, Rochester, MN 55905, USA*

† Electronic Supplementary Information (ESI) available: Supporting Information. See DOI: 10.1039/b000000x/

References

1 (a) G. M. Whitesides, *Nature*, 2006, **442**, 368. (b) G. M. Whitesides, *Nat. Biotechnol.*, 2003, **21**, 1161. (c) Y. Nakayama, P. J. Pauzauskie, A. Radenovic, R. M. Onorato, R. J. Saykally, J. Liphardt and P. Yang, *Nature*, 2007, **447**, 1098.

2 (a) T. Tagami, J. P. May, M. J. Ernsting and S. D. Li, *J. Control. Release*, 2012, **161**, 142. (b) R. Gui, A. Wan, X. Liu and H. Jin, *Chem. Commun.*, 2014, **50**, 1546.

3 (a) F. Danhier, E. Ansorena, J. M. Silva, R. Coco, A. Le Breton and V. Preat, *J. Control. Release*, 2012, **161**, 505. (b) R. C. Mundargi, V. R. Babu, V. Rangaswamy, P. Patel and T. M. Aminabhavi, *J. Control. Release*, 2008, **125**, 193. (c) X. Gong, *RSC Adv.*, 2014, **4**, 54494.

4 (a) R. Gui, H. Jin, X. Liu, Z. Wang, F. Zhang, J. Xia, M. Yang and S. Bi, *Chem. Commun.*, 2014, **50**, 14847. (b) R. Gui, A. Wan, X. Liu, W. Yuan and H. Jin, *Nanoscale*, 2014, **6**, 5467.

5 (a) Y. Wang, R. Guo, X. Cao, M. Shen and X. Shi, *Biomaterials*, 2011, **32**, 3322. (b) J. Zhu and X. Shi, *J. Mater. Chem.*, 2013, **1**, 4199.

6 X. Liu and S. Wang, in *Encyclopedia of Biomedical Polymers and Polymeric Biomaterials*, ed. M. Mishra, Taylor & Francis, New York, USA, 2014, DOI:10.1081/E-EBPP-120051253

7 (a) L. Cai, C. J. Foster, X. Liu and S. Wang, *Polymer*, 2014, **55**, 3836. (b) R. Qi, S. Liu, J. Chen, H. Xiao, L. Yan, Y. Huang and X. Jing, *J. Control. Release*, 2012, **159**, 251. (c) H. Xiao, H. Song, Y. Zhang, R. Qi, R. Wang, Z. Xie, Y. Huang, Y. Li, Y. Wu and X. Jing, *Biomaterials*, 2012, **33**, 8657.

8 M. Henry, L. Cai, X. Liu, L. Zhang, J. Dong, L. Chen, Z. Wang and S. Wang, *Langmuir*, 2015, **31**, 2851.

9 (a) A. Guiseppi-Elie, C. Dong and C. Z. Dinue, *J. Mater. Chem.*, 2012, **22**, 19529. (b) C. N. Kotanen, A. N. Wilson, C. Dong, C. Z. Dinu, G. A. Justin and A. Guiseppi-Elie, *Biomaterials*, 2013, **34**, 6318.

10 (a) J. P. Fisher, T. A. Holland, D. Dean, P. S. Engel and A. G. Mikos, *J. Biomater. Sci. Polym. Ed.*, 2001, **12**, 673. (b) S. Wang, L. Lu and M. J. Yaszemski, *Biomacromolecules*, 2006, **7**, 1976. (c) R. A. Thibault, L. Scott Baggett, A. G. Mikos and F. K. Kasper, *Tissue Eng. Part A.*, 2010, **16**, 431.

11 X. Liu, A. L. Miller II, B. E. Waletzki, M. J. Yaszemski and L. Lu. *RSC Adv.*, 2015, **5**, 21301

12 J. Yan, J. Li, M. B. Runge, M. Dadsetan, Q. Chen, L. Lu and M. J. Yaszemski, *J. Biomater. Sci. Polym. Ed.*, 2011, **22**, 489.

13 (a). S. He, M. D. Timmer, M. J. Yaszemski, A. W. Yasko, P. S. Engel and A. G. Mikos, *Polymer*, 2001, **42**, 1251. (b). L. Cai and S. Wang, *Biomaterials*, 2010, **31**, 7423.

14 (a) F. Danhier, E. Ansorena, J. M. Silva, R. Coco, A. Le Breton and V. Préat, *J. Control. Release*, 2012, **161**, 505. (b) N. Kamaly, Z. Xiao, P. M. Valencia, A. F. Radovic-Moreno and O. C. Farokhzad, *Chem. Soc. Rev.*, 2012, **41**, 2971. (c) C. Wischke and S. P. Schwendeman, *Int. J. Pharm.*, 2008, **364**, 298. (d) C. He, S. W. Kim and D. S. Lee, *J. Control. Release*, 2008, **127**, 189. (e) H. Xiao, H. Song, Q. Yang, H. Cai, R. Qi, L. Yan, S. Liu, Y. Zheng, Y. Huang, T. Liu and X. Jing, *Biomaterials*, 2012, **33**, 6507.

15 (a) L. Cai, R. E. Dewi and S. C. Heilshorn, *Adv. Funct. Mater.*, 2015, **25**,1344. (b) Z. Tao, G. Hong, C. Shinji, C. Chen, S. Diao, A. L. Antaris, B. Zhang, Y. Zou and H. Dai, *Angew. Chem.*, **125**, 13240. (c) L. Cai and S. C. Heilshorn, *Acta Biomater.*, 2014, **10**, 1751. (d) H. Xiao, W. Li, R. Qi, L. Yan, R. Wang, S. Liu, Y. Zheng, Z. Xie, Y. Huang and X. Jing, *J. Control. Release*, 2012, **163**, 304.

16 (a) Z. Yu, R. M. Schmaltz, T. C. Bozeman, R. Paul, M. J. Rishel, K. S. Tsosie and S. M. Hecht, *J. Am. Chem. Soc*., 2013, **135**, 2883. (b) B. R. Schroeder, M. I. Ghare, C. Bhattacharya, R. Paul, Z. Yu, P. A. Zaleski, T. C. Bozeman, M. J. Rishel and S. M. Hecht, *J. Am. Chem. Soc*., 2014, **136**, 13641. (c) O. C. Farokhzad, J. J. Cheng, B. A. Teply, I. Sherifi, S. Jon, P. W. Kantoff, J. P. Richie and R. Langer, *Proc. Natl. Acad. Sci. U. S. A.*, 2006, **103**, 6315. (d) Z. Zhang, S. H. Lee and S. S. Feng, *Biomaterials*, 2007, **28**, 1889. (e) C. Bhattacharya, Z. Yu, M. J.Rishel and S. M. Hecht, *Biochemistry*, 2014, **53**, 3264.

17 (a) S. D. Weitman, R. H. Lark, L. R. Coney, D. W. Fort, V. Frasca, V R. Zurawski and B. A. Kamen, *Cancer Res*., 1992, **52**, 3396. (b) J. F. Ross, P. K. Chaudhuri and M. Ratnam, *Cancer*, 1994, **73**, 2432. (c) Y. Lu and P. S. Low, *Adv. Drug Deliv. Rev.*, 2002, **54**, 675. (d) N. Parker, M. J. Turk, E. Westrick, J. D. Lewis, P. S. Low and C. P. Leamon, *Anal. Biochem*., 2005, **338**, 284.

18 D. Pan, Z. Hu, F. Qiu, Z. L. Huang, Y. Ma, Y. Wang, L. Qin, Z. Zhang, S. Zeng and Y. H. Zhang, *Nat. Commun.*, 2014, **5**, 5573.

19 Z. Wu and L. Meng, *Prog. Chem.*, 2007, **19**, 1381.

20 S. Wang, D. H. Kempen, M. J. Yaszemski and L. Lu, *Biomaterials*, 2009, **30**, 3359.

21 A. O. Saeed, S. Dey, S. M. Howdle, K. J. Thurecht and C. Alexander, *J. Mater. Chem*., 2009, **19**, 4529.

22 S. Ji, Z. Zhu, T. R. Hoye and C. W. Macosko, *Macromol. Chem. Phys.*, 2009, **210**, 823.

23 R. Yang, F. Meng, S. Ma, F. Huang, H. Liu and Z. Zhong, *Biomacromolecules*, 2011, **12**, 3047.

24 (a) I. Moreno-Villoslada, M. Jofré, V. Miranda, P. Chandía, R. González, S. Hess, B. L. Rivas, C. Elvira, J. S. Román, T. Shibue and H. Nishide, *Polymer*, 2006, **47**, 6496. (b) C. Jian, C. Gong, S. Wang, S. Wang, X. Xie, Y. Wei and J. Yuan, *Eur. Polym. J.*, 2014, **55**, 235.

25 L. Liu, K. T. Yong, I. Roy, W. C. Law, L. Ye, J. Liu, J. Liu, R. Kumar, X. Zhang and P. N. Prasad, *Theranostics*, 2012, **2**, 705.

26 W. Liu, S. Wen, M. Shen and X. Shi, *New J. Chem.*, 2014, **38**, 3917.

27 (a) Y. Lu, E. Sega, C. P. Leamon and P. S. Low, *Adv. Drug Deliv. Rev*., 2004, **56**, 1161. (b) W. Xia and P. S. Low, *J. Med. Chem.*, 2010, **53**, 6811. (c) C. P. Leamon and J. A. Reddy, *Adv. Drug Deliv. Rev.*, 2004, **56**, 1127.

28 (a) A. R. Hilgenbrink and P. S. Low, *J. Pharm. Sci.*, 2005, **94**, 2135. (b) S. Jaracz, J. Chen, L. V. Kuznetsova and I. Ojima, *Bioorg. Med. Chem*., 2005, **13**, 5043. (c) C. P. Leamon, *Curr. Opin. Investig. Drugs*, 2008, **9**, 1277. (d) P. S. Low, W. A. Henne and D. D. Doorneweerd, *Acc. Chem. Res*., 2008, **41**, 120.

29 (a) A. Gabizon, H. Shmeeda, A. T. Horowitz and S. Zalipsky, *Adv. Drug Deliv. Rev*., 2004, **56**, 1177. (b) A. K. Patri, J. F. Kukowska-Latallo and J. R. Baker Jr, *Adv. Drug Deliv. Rev.*, 2005, **57**, 2203.